The essential role of *Dnmt1* in gametogenesis in the large milkweed bug *Oncopeltus fasciatus*

Joshua T. Washington[1], Katelyn R. Cavender[1], Ashley U. Amukamara[1], Elizabeth C. McKinney[1], Robert J. Schmitz[2], Patricia J. Moore[1,*]

[1] Department of Entomology, University of Georgia

[2] Department of Genetics, University of Georgia

*Patricia J. Moore, 413 Biological Sciences Building, Department of Entomology, University of Georgia, Athens, GA, 30602; (706) 542-0169

Email: pjmoore@uga.edu

Patricia J. Moore: https://orcid.org/0000-0001-9802-7217

Robert J. Schmitz: https://orcid.org/0000-0001-7538-6663

Keywords

DNA methylation, epigenetics, *Dnmt1*, spermatogenesis, germ cells, *Oncopeltus fasciatu*

Abstract

Given the importance of DNA methylation in protection of the genome against transposable elements and transcriptional regulation in other taxonomic groups, the diversity in both levels and patterns of DNA methylation in the insects raises questions about its function and evolution. We show that the maintenance DNA methyltransferase, DNMT1, affects meiosis and is essential to fertility in milkweed bugs, *Oncopeltus fasciatus*, while DNA methylation is not required in somatic cells. Our results support the hypothesis that *Dnmt1* is required for the transition of germ cells to gametes in *O. fasciatus* and that this function is conserved in male and female gametogenesis. They further suggest that DNMT1 has a function independent of DNA methylation in germ cells. Our results raise the question of how a gene so critical in fitness across multiple insect species can have diverged widely across the insect tree of life.

13 **Introduction**

14 Despite the apparent ubiquity of DNA methylation across the eukaryotic tree of life (Schmitz et
15 al. 2019, Lewis et al. 2020), in the insects there is considerable variation both in the presence and
16 extent of DNA methylation and even the presence and number of the DNA methyltransferases
17 (Bewick et al. 2016, Lyko 2018, Glastad et al. 2019). Thus, the functional role of DNA
18 methylation and its associated DNA methyltransferases in the insects is unclear. While some
19 studies have associated levels of methylation with gene expression, most studies in the insects
20 find no functional association (Bewick et al. 2016, Glastad et al. 2019).

21 One role emerging from knockdown and silencing studies across several insect species is that
22 *Dnmt1* is required for oogenesis (Schulz et al. 2018, Bewick et al. 2019, Gegner et al. 2019,
23 Amukamara et al. 2020). For example, *Dnmt1* is required for maintenance of DNA methylation
24 following cell division in the milkweed bug, *Oncopeltus fasciatus* (Bewick et al. 2019,
25 Amukamara et al. 2020), the downregulation of *Dnmt1* using RNAi results in a reduction in
26 methylation and also the cessation of oogenesis. However, it is unclear whether the effect on
27 oogenesis is mediated by the reduction in DNA methylation (Amukamara et al. 2020). While the
28 expected reduction in DNA methylation is seen throughout the organism following *Dnmt1*
29 knockdown, the only phenotypic consequence is to the germ cells. Evidence from other species
30 supports a function independent of DNA methylation. *Dnmt1* is also essential to egg production
31 in *T. castaneum* (Schulz et al. 2018), a beetle that has no DNA methylation at all (Zemach et al.
32 2010). This suggests that *Dnmt1* can have a function specific to germ cells in insects that is
33 independent of its function in maintaining DNA methylation. This led us to hypothesize that
34 *Dnmt1* plays a role in meiosis in insects (Amukamara et al. 2020).

35 In this study, we tested the hypothesis that *Dnmt1* is essential to gametogenesis in *O. fasciatus*.
36 Furthermore, if *Dnmt1* has a role in gametogenesis, including meiosis, it should be conserved
37 across the sexes. Testing the function of *Dnmt1* in males allows us to capitalize on the well-
38 characterized process of spermatogenesis in *O. fasciatus*, specifically (illustrated in Figure 1;
39 Economopoulos & Gordon 1971), and the conserved features of insect spermatogenesis,
40 generally (Dallai 2014). In *O. fasciatus,* as in many insects, there are two points in development
41 where meiosis can occur. The first stage where meiosis will occur is during the larval stages.
42 Testis development and spermatogenesis is initiated during larval development in *O. fasciatus*
43 (Economopoulos & Gordon 1971). During the first three instars the testes consist of seven
44 globular follicles that will develop into the testis tubules (Schmidt et al. 2002). Meiosis is
45 initiated in the 4th instar, and by the end of the 4th instar, cysts containing spermatids are present.
46 Differentiation of the spermatids commences in the 5th instar, and males emerge with up to
47 250,000 spermatids that continue to differentiate during sexual maturation. Thus, we can target
48 the developmental time point at which meiosis occurs. In addition, *O. fasciatus* males can
49 produce gametes throughout their adult lives and therefore meiosis can occur in the adult testis.
50 If *Dnmt1* is required for meiosis and gametogenesis we predicted that it will be required both
51 during larval development and as adult males replenish sperm stores following mating. We
52 therefore compared the testis phenotypes of adults developing from nymphs in which *Dnmt1*
53 expression was downregulated either before or after the major wave of meiosis that occurs in
54 testis development (Economopoulos & Gordon 1971, Schmidt et al. 2002, Ewen-Campen et al
55 2013). We also treated sexually mature adults, and examined fertility in males following sperm
56 depletion, testing for the ability of knockdown males to replenish sperm stores following
57 multiple matings. Our results demonstrated that expression of *Dnmt1* is required for the

58 development of sperm both during larval and adult spermatogenesis and that the impact of
59 *Dnmt1* knockdown was greatest if it occurred prior to the onset of meiotic divisions in the
60 developing testes. These results establish that *Dnmt1* plays a critical conserved function across
61 the sexes during gametogenesis in *O. fasciatus* and that it is required for germ cell development.

62 **Results**

63 **The pattern of *Dnmt1* expression during testis development and across tissues suggests a**
64 **role in spermatogenesis.**

65 We measured *Dnmt1* expression during larval development and sexual maturation. Our
66 prediction was that if *Dnmt1* is required during gametogenesis, particularly meiosis, then its
67 expression should mirror those of two genes known to be involved in germ cell development,
68 *Boule* and *Vasa* (Shah et al. 2010, Yajima & Wessel 2011). Thus, we predicted that *Dnmt1*
69 expression would be highest during the stages when gametogenesis is occurring. As predicted,
70 testis-specific expression of *Dnmt1* is highest during the 4th and 5th instars of development
71 (Figure 2A; ANOVA, $F = 27.426$, d.f. = 3, 38, $p < 0.001$), stages when meiosis and
72 spermatogenesis is most active (Economopoulos & Gordon 1971). The expression is lowest in
73 virgin adult males. This expression pattern mirrored that observed for *Boule*, a gene with a well-
74 characterized role in meiosis (Figure 2B; ANOVA, $F = 36.346$, d.f. = 3, 38, $p < 0.001$). *Dnmt1*
75 expression pattern was also similar to *Vasa*, a highly conserved marker of the germline (Figure
76 2C; ANOVA, $F = 20.444$, d.f. = 3, 38, $p < 0.001$). While *Dnmt1* is expressed across all adult
77 tissues, as would be expected given its role in maintenance of DNA methylation, expression is
78 highest in testes compared to gut, head, and muscle tissue (Figure 2-figure supplement 1;
79 ANOVA, $F = 67.311$, d.f. = 3, 36, $p < 0.001$), also suggesting a special role during
80 gametogenesis.

81 ***Dnmt1* knockdown reduced levels of DNA methylation in the testis genome**.

82 To confirm the effectiveness of our RNAi treatment, we measured expression of *Dnmt1* in a
83 subset of ds-RED and ds-*Dnmt1* injected males (Figure 3). Quantitative PCR demonstrated
84 reduced levels of *Dnmt1* mRNA in ds-*Dnmt1* injected males compared to ds-RED injected males
85 in both 3rd instar (ANOVA; $F = 83.126$, d.f. = 1, 31, $p < 0.001$) and 5th instar (ANOVA; $F =$
86 49.793, d.f. = 1, 22, $p < 0.001$) treated males 6 to 10 days following injection with dsRNA.
87 Treatment of males with ds-*Dnmt1* had the predicted effect on *Dnmt1* function in maintenance of
88 methylation. We performed whole genome bisulfite sequencing to evaluate the impact of the ds-
89 *Dnmt1* on DNA methylation genome wide. The reduction in expression of *Dnmt1* in the RNAi
90 individuals had the expected phenotypic effect on DNA methylation with a reduction of genome
91 methylation in the testes for ds-*Dnmt1* treated males, but not control males (Figure 3-figure
92 supplement 1). Genomic DNA from the testes of control treated males had approximately 12.5%
93 CpG methylation regardless of stage they were treated. Knockdown of *Dnmt1* at the earlier stage
94 of development led to a greater percentage reduction of methylation. Treatment with ds-*Dnmt1* at
95 the 5th instar reduced the percent CpG methylation from around 12.5% to around 5%. Treatment
96 with ds-*Dnmt1* at the 3rd instar reduced the level of methylation even further, to around 2%, as
97 predicted given the greater numbers of cell divisions that were expected between treatment and
98 sampling between these two treatments.

99 ***Dnmt1* knockdown affected testis size and structure.**

100 Knockdown of *Dnmt1* prior to meiosis, in the 3rd instar stage, had a significant effect on testis
101 size in virgin males, while knockdown of *Dnmt1* during the developmental stage after which
102 meiosis is initiated, the 5th instar stage, had no effect on testis size (Figure 4; ANOVA, $F =$
103 20.360, d.f. = 4, 58, $p < 0.001$) compared to either uninjected controls or ds-RED treated males.

104 Knockdown of *Dnmt1* prior to meiosis affected testis tubules to a greater extent than knockdown
105 following the initiation of meiosis during larval testis development (Figure 5). Control males
106 injected in the 3rd or 5th instar stage of development showed the expected structure of the testis
107 tubule (Figure 5A and C). At the anterior end of the testis tubule, spermatogonia and primary
108 spermatocytes had the characteristic nuclear structure and there was clear evidence of mitotic
109 division within the spermatogonia (Figure 5C, arrowhead), using α-phosphohistone H3 (pHH3)
110 to stain for chromosome condensation in preparation for mitosis and meiosis. We also observed
111 α-pHH3 staining in spermatocysts at the border between primary and secondary spermatocytes
112 in the control testis tubules in both 3rd and 5th instar treated males. Following this band of
113 relatively synchronous meiotic activity, the posterior testis tubule showed spermatids and
114 developing spermatozoa as they matured. We confirmed the use of this band of α-pHH3 stained
115 spermatocysts as a landmark of meiosis using knockdown of *Boule* (Figure 5-figure supplement
116 1).

117 The structure of the testis tubules of males treated with ds-*Dnmt1* in the 3rd instar was highly
118 disrupted and both the anterior and posterior testis tubule was affected (Figure 5B). There were
119 fewer spermatocysts in both the region of spermatogonia and primary spermatocytes. While
120 there were occasional α-pHH3 positive nuclei, these were not well organized into spermatocysts
121 and were spread throughout the testis tubule rather than organized at the junction between
122 primary and secondary spermatocytes. There was evidence of mitotic activity in the
123 spermatogonia (Figure 5B arrowhead), although these were less frequent in ds-*Dnmt1* treated
124 males than control males. The testis tubules of males treated with ds-*Dnmt1* in the 5th instar stage
125 of development had a structure much more similar to control males (Figure 5D). Mitotic activity
126 was apparent in the spermatogonia (Figure 5D arrowhead) and most testis tubules had evidence

127 of mature sperm and α-pHH3 stained spermatocysts at the junction between primary and
128 secondary spermatocytes (Figure 5D arrow). Unorganized spermatocysts below this junction
129 were frequently observed, however, and ds-*Dnmt1* males treated at the 5th instar had variable
130 phenotypes posterior to the primary spermatocytes, presumably depending on when treatment
131 occurred following the wave of meiosis along the testis tubule axis.

132 ***Dnmt1* knockdown in adult males prevented replenishment of sperm stores**

133 Downregulating *Dnmt1* expression in adult males resulted in a loss of fecundity over time. The
134 third and final females mated to ds-*Dnmt1* treated males ran out of sperm to fertilize eggs more
135 rapidly than those mated to control males. Clutches of eggs laid by females mated to ds-*Dnmt1*
136 treated males were not fertilized and failed to hatch at an earlier collection day than those laid by
137 females mated to control males (Figure 6; Wilcoxon $\chi^2 = 13.978$, d. f. = 1, $p < 0.001$).

138 The loss of fertility in males was associated with smaller testis size. Males treated with ds-*Dnmt1*
139 at seven days post-emergence and then allowed to mate for three weeks prior to dissection had
140 statistically significantly smaller testis area than the testes of control males after the same mating
141 treatment (ANOVA, F = 29.084, d.f. = 1, 51, $p < 0.001$; Figure 6-figure supplement 1). The
142 smaller testis area of ds-*Dnmt1* treated adult males was associated with a breakdown in testis
143 tubule structure and the loss of sperm from the testis tubules (Figure 7). In control males, three
144 weeks post injection the regions of spermatogenesis were recognizable. Small spermatocysts
145 with spermatogonia undergoing mitotic divisions were observable at the anterior tip of the testis
146 tubule (Figure 7A and B). Posterior to the spermatogonia were the primary spermatocytes with
147 more diffuse nuclear structure. We often observed the band of α-pHH3 positive spermatocysts
148 that indicated the first meiotic division to form the secondary spermatocytes. At the most
149 posterior end of the testis tubule the spermatids developed into spermatozoa. Three weeks after

150 *Dnmt1* knockdown testis tubule structure is significantly disrupted. There appeared to be fewer
151 spermatogonia and those that remained had a more condensed nuclear structure than in the testis
152 tubules of control males (Figure 7C and D). The most noticable effect was seen in the region
153 containing the spermatocytes. There were few primary spermatocytes in the testis tubule and α-
154 pHH3 positively stained spermatocysts were rarely observed, indicating few spermatocysts
155 undergoing meiosis.

156 **Discussion**

157 The function of DNA methylation and the DNA methylation enzymes across the insect tree of
158 life has been widely debated, particularly in light of the extreme variation in presence of this
159 chromatin modification and the diversification of the enzymatic toolkit required to methylate
160 DNA *de novo* and maintain DNA methylation patterns (Bewick et al. 2016, Lyko 2018, Lewis et
161 al. 2020). This evolutionary pattern is particularly intriguing given that in two species on
162 divergent branches of the insect phylogeny the maintenance methyltransferase DNMT1 is
163 essential to gametogenesis, and thus is tightly tied to fitness, even in a species where DNA
164 methylation itself is absent (Schulz et al. 2018). While functional studies have not been done in
165 other species, a summary of expression studies on the DNA methyltransferases across a diversity
166 of insects suggest that these enzymes could be involved in gametogenesis across a number of
167 species, ranging from fire ants, *Solenopsis invicta* (Kay et al. 2018), to jewel wasps, N*asonia*
168 *vitripennis* (Zwier et al. 2012), to migratory locusts, *Locusta migratoria* (Robinson et al. 2016),
169 and the brown plant hopper, *Nilaparvata lugens* (Zhang et al. 2015). Here we showed that *Dnmt1*
170 expression affects germ cell development. The effect of downregulating *Dnmt1* in males, as in
171 females (Amukamara et al. 2020), was specific to the germ cells. The downregulation of *Dnmt1*
172 did result in reduction of DNA methylation, but there were no obvious morphological impacts to

173 the RNAi-treated individuals. Our results show that the function of *Dnmt1* in germ cells is
174 conserved across the sexes within a species, and other results document that *Dnmt1* expression is
175 required for oogenesis among species. This raises a conundrum when we look across the insect
176 tree of life. How can a gene required for such a fundamental fitness activity in examples from
177 such a diverse group of insects also be so evolutionarily labile? This suggests that the function
178 *Dnmt1* in germ cell development is easily lost or replaced.

179 ***Dnmt1* knockdown causes inhibition of spermatogenesis consistent with a role in meiosis**

180 If our hypothesis on the role of *Dnmt1* in meiosis is correct, then spermatogenesis should be
181 affected by *Dnmt1* expression as well as oogenesis, as it is a shared process across
182 gametogenesis during sexual reproduction. In the testes *O. fasciatus* males, we observed both
183 spermatogonia and primary spermatocytes that stain positively for phosphorylation of the serine
184 10 residue of histone protein H3. While the pattern of histone H3 phosphorylation across meiosis
185 has not been specifically studied in *O. fasciatus*, phosphorylation of the serine 10 is typically
186 associated with chromosome condensation during meiosis (Hans and Dimitrov 2001) and mitosis
187 (Prigent and Dimitrov 2003). Moreover, the pattern of α-pHH3 staining along the axis of the
188 testis tubule is consistent with this histone modification occurring in both mitosis and meiosis.
189 We observed α-pHH3 positive cells both within spermatocysts containing the mitotically
190 dividing spermatogonia and also at the boundary between primary and secondary spermatocytes.
191 We have confirmed this landmark using *Boule* knockdown males. In *Drosophila*, *Boule* is
192 required for progression of spermatocytes through meiosis. Germ cells lacking functional *Boule*
193 become arrested at meiotic prophase (Eberhart et al. 1996). In the testes of *O. fasciatus* males
194 treated with ds-*Boule*, the affected cells were all posterior to the band of synchronous α-pHH3
195 positive spermatocytes. Thus, α-pHH3 staining provided a landmark for entry into meiosis.

196 We did not see the band of α-pHH3 positive spermatocysts at the border between primary and
197 secondary spermatocytes in the *Dnmt1* knockdown males treated at the 3rd instar stage of
198 development. This could be interpreted as the primary spermatocytes have not initiated
199 chromosome condensation. However, we did observe individual α-pHH3 positive nuclei in the
200 posterior testis tubule. So there could have been arrest after chromatin condensation with a
201 breakdown in spermatocyst structure. Interestingly, the testis phenotype of our *Dnmt1*
202 knockdown males resembled the phenotypic effect of *Vasa* knockdown reported by Ewen
203 Campen et al. 2013. *Vasa* RNAi results in defects in cyst integrity and Ewen Campen et al.
204 (2013) propose that *Vasa* plays a specific role in the onset or synchrony of meiosis. *Vasa* has also
205 been proposed to be required for the correct progression through meiosis in mice (Tanaka et al.
206 2000) and humans (Medrano et al. 2012). Thus, the phenotypic similarity between *Dnmt1*
207 knockdown and *Vasa* knockdown testes in *O. faciatus* support the hypothesis that *Dnmt1* may be
208 required for the successful initiation and completion of meiosis in spermatocytes. More work
209 remains to determine exactly what stage of sperm development is impacted by the decrease in
210 *Dnmt1* expression.

211 The phenotype of knockdown of *Dnmt1* is exacerbated when knockdown occurs prior to the
212 stage of testis development when meiosis occurs. This result is consistent with what was
213 observed in female *O. fasciatus* (Amukamara et al. 2020) in which knockdown of *Dnmt1*
214 expression prior to the stage of oocyte development inhibited all oocyte formation. One
215 interpretation of this result is that *Dnmt1* is required for successful progression through meiosis.
216 However, it is clear that reducing *Dnmt1* expression had an impact beyond simply reducing the
217 ability to enter or complete meiosis. A block to progression through meiosis, as demonstrated by
218 the *Boule* knockdown, spermatogonia and primary spermatocytes would continue to be born but

219 remain viable after a failure to complete meiosis. In the *Dnmt1* knockdowns, however, there
220 were fewer germ cells of any type, and those that remained in the testis tubule often appeared to
221 have abnormal and condensed nuclei. It remains to be determined if *Dnmt1* is required for
222 meiosis or if the association with meiosis is a correlation; *Dnmt1* could be required for viability
223 of germ cells and act at the stage of development at which they would be undergoing meiosis.

224 Previous studies on the function of *Dnmt1* in insect spermatogenesis have not documented any
225 effect on male fertility. Knockdown of *Dnmt1* in the red flour beetle, *T. castaneum* (Schulz et al.
226 2018) had no effect on the fecundity of female mating partners was measured in the first nine
227 days post mating and the authors conclude that *Dnmt1* is not required for spermatogenesis in *T.*
228 *castaneum*. We suspect that the function of *Dnmt1* in spermatogenesis is not unique to *O.*
229 *fasciatus*, given the expression patterns of *Dnmt1* in other insects (Robinson et al. 2016, Kay et
230 al. 2018). In the *T. castaneum* study, the authors did not examine testis structure or design a
231 mating strategy that would exhaust the sperm stores of the males and so may have missed a
232 fertility effect. In holometabolous insects, including beetles, spermatocytes are typically formed
233 by the end of larval development (Economopoulos & Gordon 1971), thus males treated as pupae
234 would still emerge with large numbers of sperm in their testes. Here we showed that male *O.*
235 *fasciatus* treated with ds-*Dnmt1* RNA as sexually mature adults become sperm limited more
236 rapidly than control males. There is a potential alternative explanation, that *Dnmt1* knockdown
237 males could continue to produce sperm but that sperm was of low quality and unable to support
238 development. Given that the testes of ds-*Dnmt1* treated males were significantly smaller than
239 control males and had altered testis tubule structure, which indicated that spermatogenesis was
240 significantly impacted, we concluded that *Dnmt1* knockdown males are unable to replenish
241 sperm supplies. The functional role of *Dnmt1* in testes across other species remains to be tested.

242 **DNA methylation and germ cell development**

243 The knockdown of *Dnmt1* resulted in a reduction of DNA methylation within the testes, as
244 predicted. The effect was greater in the nymphs that were treated in an earlier stage of
245 development, as would be expected given the greater number of cell divisions that would occur
246 between treatment and collection of the testes between the 3rd and 5th instar treatments. The more
247 extreme phenotype in the 3rd instar treated males could be explained by the greater reduction in
248 methylated CpG. However, the percent methylation seen in the testes of the 5th instar ds-*Dnmt1*
249 treated males was similar to that seen in females treated at the 4th instar stage of development
250 (Amukamara et al. 2020), greater than a two-fold reduction in the percent methylated CpG
251 residues. In *Dnmt1* knockdown females, there was a compete loss of oocyte production when
252 DNA methylation was reduced to this level while in males the phenotype of the 5th instar *Dnmt1*
253 knockdowns was close to normal. This disconnect between reduction of DNA methylation and
254 phenotypic effects mirrors what has been seen in the beetle, *T. castaneum* (Schulz et al. 2018). In
255 this species, the reduction of DNA methylation is an evolved difference rather than an
256 experimental effect, but the results are similar to what we have observed in *O. fasciatus*; DNA
257 methylation is not required for function of somatic cells, but downregulation of *Dnmt1*
258 expression leads to specific germ cell effects. The lack of correlation between extent of
259 methylation and function in germ cells strengthens our hypothesis that there may be a pleiotropic
260 function for *Dnmt1* in germ cells that acts independently of DNA methylation levels.
261 Alternatively, DNA methylation may have a specific role in the germ cells that it does not play in
262 somatic cells. Perhaps DNA methylation is required for proper gene expression in germ cells or
263 it may be required for transposon silencing only in germ cells. However, demethylation of
264 ovarian tissue in *O. fasciatus* showed little relationship between methylation levels and gene

265 expression, with few differentially transcribed genes (Bewick et al. 2019). Another possibility is
266 that DNA methylation state may be a prerequisite for successful completion of meiosis and not
267 mitosis. For example, *O. fasciatus* has holocentric chromosomes and undergoes inverted meiosis
268 (Viera et al. 2009). During mitosis chromosomes have a kinetocore that extends across the
269 majority of the chromosome but in meiosis, the kinetochore plate is missing and microtubules
270 extend into the chromosome (Comings & Okada 1972). One could imagine that DNA
271 methylation might be required for this interaction. However, the complete lack of methylation
272 but a functional role of *Dnmt1* in *T. casteneum* oogenesis alongside our results argues for a
273 pleiotropic function for *Dnmt1* in gametogenesis that is independent of its role in DNA
274 methylation.

275 Conclusion

276 *Dnmt1* expression is required for germ cell development in both male and female *O. fasciatus*.
277 The block to germ cell development in *Dnmt1* knockdowns appeared to be associated with
278 meiosis, although it was not a simple block to progression through meiosis as germ cells are lost
279 from the testes. Thus, *Dnmt1* may be required for germ cell viability. It still remains to be
280 determined if the block in gametogenesis depends on DNA methylation or an alternative
281 function of *Dnmt1*, as suggested by the requirement for *Dnmt1* during gametogenesis in an insect
282 with a non-methylated genome (Schultz et al. 2018). Whatever the specific function of *Dnmt1* in
283 gametogenesis, the requirement for this enzyme in such a critical fitness function as the
284 production of gametes in representatives of different groups of insects raises important questions
285 as to how this enzyme and the entire methylation toolkit has evolved across the insect tree of life
286 (Lyko et al 2018, Provataris et al. 2018). Functional analysis of *Dnmt1* in the insect groups
287 where it is found, and study of how these functions are replaced in the species where it is no

288 longer found, will be essential for understanding the evolution of this important base

289 modification.

290 **Materials and Methods**

Key Resources Table				
Reagent type (species) or resource	**Designation**	**Source or reference**	**Identifiers**	**Additional information**
strain, strain background	*Oncopeltus fasciatus*	Carolina Biologicals	Item # 143810 NCBI Taxon:7535	Cultured in Moore lab for 5 years
antibody	anti-phospho-Histone H3 (Ser10) (Rabbit polyclonal)	Millipore	Cat # 06-570 RRID:AB_310177	IF (1:1000)
commercial assay or kit	Qiagen RNA easy kit with Qiazol	Qiagen	Cat # 74104	
commercial assay or kit	LightCycler 480 SYBR Green I Master	Roche	Product No. 04707516001	
commercial assay or kit	MEGAscript T7 Transcription kit	ThermoFisher Scientific	AMB13345	
sequence-based reagent	ds-*Dnmt1* RNAi primer set for transcription template	Amukamara et al. 2020	PCR primers	Sense: TGATGCTCG GCCTCAAAAC AAGAT Anti-sense: ACTCCAGGA GGTGGAACA GTAGTCT

sequenced-based reagent	ds-*Boule* RNAi primer set for transcription template	Amukamara et al. 2020	PCR primers	Sense: AGCCTCACCA CCAGTATTCG Anti-sense AGGGTGCCT AGGATTGGA CT
sequenced-based reagent	qRT-PCR primer set: *Dnmt1*	Amukamara et al. 2020	PCR primers	Sense: GCTTGGACA AAGGCTACT ACT Anti-sense: CTTCGTGGTC CCTTATCCTT ATC
sequenced-based reagent	qRT-PCR primer set: *Boule*	Amukamara et al. 2020	PCR primers	Sense: TATTCGTACC ACCCTCTTCC Anti-sense: GACAATGGC TGGGTCATA AG
sequenced-based reagent	qRT-PCR primer set: *Vasa*	Amukamara et al. 2020	PCR primers	Sense: CTGTTGCTCC TCAGGTTAT T Anti-sense: CATTAAGCCT TCCAGGAGT AG
sequenced-based reagent	qRT-PCR primer set: *actin*	Amukamara et al. 2020	PCR primers	Sense: CTGTCTCCCG AAAGAGAAT ATG Anti-sense: TCTGTATGG ATTGGAGGA TCTA
sequenced-based reagent	qRT-PCR primer set: *GAPDH*	Amukamara et al. 2020	PCR primers	Sense: ACGGTTTCA AGGAGAAGT TAG Anti-sense: AGCTGATGG

				TGCAGTTATG
software, algorithm	JMP Pro	SAS Institute	Version 14.1 RRID:SCR_014242	
other	DAPI stain	Invitrogen	D1306	0.5 µg/mL

291 **Animal care**

292 All experimental animals were from colonies of laboratory reared *O. fasciatus* (Carolina
293 Biologicals, Burlington, NC) and were reared under standard rearing conditions of 12 hr:12 hr
294 light/dark at 27° C. To collect animals of known age and social conditions, eggs were removed
295 from the mass colonies and allowed to hatch in plastic storage containers containing *ad libitum*
296 deionized water and organic, raw sunflower seeds. For the nymph injections, nymphs were
297 pulled from mixed sex nymph colonies at the 3rd instar or 5th instar. For adult injections, nymphs
298 were separated by sex at the 4th instar and housed in single sex colonies. These were checked
299 daily and newly emerged adults. All experimental animals were placed into individual petri
300 dishes with food and water.

301 **Developmental expression**

302 Given our hypothesis that *Dnmt1* is required for development of germ cells and meiosis we
303 examined the expression levels of *Dnmt1* across testis development in males. Groups of nymphs
304 were staged and sexed. Testes were dissected from 4th and 5th instar nymphs and flash frozen in
305 liquid nitrogen and stored at -80° C. We also collected testes from virgin males on the day of
306 adult emergence and after sexual maturation at 7 days post-adult-emergence. We also collected

307 head, gut, and muscle samples from the sexually mature adult male individuals for tissue specific
308 expression.

309 Total RNA was extracted using a Qiagen RNA easy kit with Qiazol (Qiagen, Venlo, The
310 Netherlands) and complementary DNA (cDNA) synthesized from 500 ng RNA with aScript
311 cDNA Super-Mix (Quanta Biosciences, Gaithersburg, MD). Quantitative real-time PCR (qRT-
312 PCR) was used to determine expression levels of *Dnmt1* and two genes with known functions in
313 spermatogenesis, *Boule* and *Vasa*. Primers are described in Amukamara et al. 2020. As in
314 Amukamara et al. 2020, actin and GAPDH were used as reference genes. We have previously
315 validated these reference genes and they are accepted as robust reference genes in *O. fasciatus*
316 (Meinzer et al. 2019). We used a Roche LightCycler 480 with the SYBR Green Master Mix
317 (Roche Applied Science Indianapolis, IN). All samples were run with 3 technical replicates using
318 10 μL reactions. There were 10 biological replicates for each stage. Each biological replicate of
319 2nd, $3^{rd,}$ 4th, and 5th instar nymphs consisted of pools of 10, 5, 4, and 3 individuals, respectively.
320 Adult replicates consisted of individual animals. Sample size was based on past experience
321 balanced by the cost of qRT-PCR. Primer efficiency calculations, genomic contamination
322 testing, and endogenous control gene selection were performed as described in Cunningham et
323 al. 2014. We used the ΔΔCT method to compare levels of gene expression across the samples
324 (Livak and Schmittgen 2001). Gene expression was standardized per individual to account for
325 different numbers of individuals within each group at each developmental stage. Differences in
326 expression levels were analyzed using ANOVA in JMP Pro v14. If there was a significant
327 overall effect, we compared means using Tukey-Kramer HSD.

328 **RNAi preparation**

329 Double-stranded RNAs were prepared as described in Amukamara et al. 2020. Briefly, DNA
330 templates were prepared by PCR using gene-specific primers (Amukamara et al. 2020). Sense
331 and anti-sense RNA were transcribed together with an Ambion MEGAscript kit (ThermoFisher
332 Sci, Waltham, MA) and allowed to anneal to form a 404 bp ds-*Dnmt1* RNA. The concentration
333 of dsRNA was adjusted to 3 μg/μL in injection buffer (5 mM KCl, 0.1 mM NaH_2PO_4).

334 **Nymph injections, testis size and morphology**

335 To examine the effect of *Dnmt1* knockdown prior to or following the wave of meiosis initiated in
336 the 4th instar stage, nymphs were injected with ds-*Dnmt1* or control ds-RED injections at either
337 the 3rd instar or 5th instar stage of development. For further information on controls and testing
338 for potential off-target effects please see Amukamara et al. 2020. Nymphs were anaesthetized at
339 4° C for 20 minutes prior to injection. Nymphs were injected in the abdomen using pulled glass
340 capillary needles (Sutter Instrument Company micropipette puller model P-97, Novato, CA)
341 between the third and fourth abdominal segments (Chesebro et al. 2009). Nymphs were injected
342 with 2 μL volume for all injections. Following injections, nymphs were placed in individual petri
343 dishes and monitored for development. Date of adult emergence was recorded. We did not do a
344 power analysis, but based on preliminary data on the strength of the effect we aimed for 25
345 individual males for each treatment. Males were randomly assigned to a treatment group. Not all
346 males survived to age of dissection, resulting in final sample sizes of 22 and 19 for 3rd instar
347 males injected with buffer and ds-*Dnmt1*, respectively and 25 and 20 for 5th instar males injected
348 with buffer and ds-*Dnmt1*, respectively.

349 *Testis size*: At 7 to 10 days post-adult emergence, virgin males were dissected and their testes
350 were removed. Whole testes were allowed to settle into 1 mL Phosphate Buffered Saline (PBS)
351 and were imaged with a Leica M60 Stereomicroscope with Leica Application Suite software

352 (LAS v4). Testis area was measured on one of the pair from each male with the LAS by
353 outlining the whole testis with all 7 testis tubules. Differences in testis area were analyzed using
354 ANOVA in JMP Pro v14.

355 *Testis tubule structure*: *O. fasciatus* testes contain 7 individual testis tubules surrounded by a
356 relatively impermeable, autofluorescent membrane. Individual testis tubules were removed from
357 the outer membranous sheath for fixation and staining. Males from each treatment were dissected
358 across 4 dissection days. Testis tubules from individual males within a treatment were pooled for
359 staining. Thus each day one tube was a replicate with tubules from several individual males.
360 Tubules were fixed for 30 minutes in 4% formaldehyde in PBS plus 0.1% Triton-X100 (PBT)
361 and stained for evidence of cell division using an α-phosphohistone H3 Ser10 (pHH3) primary
362 antibody (Millipore antibody 06-570, Sigma-Aldrich, St. Louis, MO). α-phosphohistone H3
363 (pHH3) stains for chromosome condensation in preparation for mitosis and meiosis (Hans &
364 Dimitrov 2001, Prigent & Dimitrov 2003). The secondary antibody was an Alexa Fluor goat-
365 anti-rabbit 647 (ThermoFisher Scientific, Waltham, MA). Following antibody staining the
366 tubules were stained with DAPI (0.5 μg/mL PBT) to visualize nucleic acids. Stained tubules
367 were mounted in Mowiol 4-88 mounting medium (Sigma-Aldrich, St. Louis, MO) and visualized
368 with an Olympus BX51 Fluorescent microscope. Images were taken of every testis tubules
369 present on each slide. Representative images are presented in the figures.

370 **Quantitative Real Time PCR**

371 While we had evidence that all our RNAi treatments successfully knocked down expression in
372 females (Amukamara et al. 2020), to confirm that our RNAi treatment was effective in males,
373 total RNA and genomic DNA was extracted from flash frozen testes of a subsample of males 6
374 to 10 days following injection with the dsRNA using a Qiagen Allprep DNA/RNA Mini Kit

375 (Qiagen, Venlo, The Netherlands). Expression levels for *Dnmt1* was analyzed using qRT-PCR as
376 described above.

377 **Quantification of DNA methylation**

378 The DNA from each prep used for qRT-PCR was used to prepare MethylC-seq libraries as
379 described in Urich et al. 2015 and Amukamara et al. 2020. Samples were sequenced on a
380 NextSeq500 and qualified reads were aligned to the *O. fasciatus* genome assembly according to
381 previously published methods (Schmitz et al. 2013). The percent DNA methylation was
382 calculated by dividing the total number of methylated CpG sites by the total number of CpG sites
383 (Schultz et al. 2012). Spiked in Lambda DNA, which is fully demethylated, was used as a control
384 for the sodium bisulfite conversion rate of unmodified cytosines. Three individuals were
385 sequenced for each treatment.

386 **Adult injections**

387 *RNAi treatment*: Sexually mature virgin males (7 days post-adult-emergence) were injected with
388 3 µL ds-*Dnmt1* RNA or control injections using a pulled glass capillary needle between the third
389 and fourth abdominal segments (Chesebro et al. 2009). Control injections for the male fecundity
390 experiments were injection buffer alone. We used ds-RED control injections for the testis
391 imaging experiment. Previous studies from our lab have shown no difference in buffer alone
392 controls or non-specific ds-RNA (Bewick et al. 2019). Following injection males were placed
393 into individual petri dishes and provided with *ad libitum* food and water. We did not do a power
394 analysis, but based on preliminary data on the strength of the effect we aimed for 30 individual
395 males for each treatment. Males were randomly assigned to a treatment group.

396 *Male fecundity*: Preliminary experiments had shown that two previous matings were required to
397 deplete sperm stores. Therefore, in order to allow males to deplete sperm stores acquired during
398 nymphal development and sexual maturation, males were placed in mating trials with three 7- to
399 10-day-old virgin females, one provided each week. The first female was placed in the male's
400 petri on the day of injection with cotton wool as an oviposition substrate. The female and all eggs
401 were removed at the end of the week (7 days post-injection) and discarded and replaced with a
402 second 7- to 10-day-old virgin female and fresh cotton wool. Again, at the end of the week (14
403 days post-injection), the female and all resulting eggs were discarded. A third, focal, 7- to 10-
404 day-old virgin female was placed with the male with fresh cotton wool. The 3rd female and
405 experimental male were given one week to mate before the male was removed from the petri
406 dish for analysis of testis size and structure. The female was maintained for her lifetime,
407 provided with *ad libitum* food and water. The eggs produced by the 3rd female were collected
408 from the petri dish twice a week at 3-4 day intervals and the oviposition substrate replaced with
409 fresh cotton wool. The eggs collected were placed in a separate container and allowed to develop
410 to hatching (approximately 7-10 days following collection) and then frozen at -20° C until
411 assayed. We recorded the first collection date for which no eggs hatched. We analyzed the time
412 to end of fertilized eggs due to sperm depletion relative to treatment using a survival analysis
413 (Wilcoxon Rank Sum test) using JMP Pro v14.1. Not all males survived to date of dissection, or
414 their mates died during the course of egg collection, requiring these males to be removed from
415 the analysis, resulting in a sample size of 21 control and 20 ds-*Dnmt1* treated males in the final
416 fecundity analysis.

417 *Testis size*: At the end of the one-week mating trial with the 3rd female (21 days post-injection),
418 males were dissected and their testes removed into 1 mL Phosphate Buffered Saline (PBS).

419 Whole testes were photographed and measured as described above. Not all males survived to
420 date of dissection, resulting in a final sample size of 28 control and 25 ds-*Dnmt1* treated males.

421 *Testis tubule structure*: Testis tubules from mated males were isolated, fixed and stained as
422 described above.

423 **Acknowledgments**

424 The authors acknowledge Allen J. Moore and other members of the Moore lab for many helpful
425 discussions. We acknowledge Luvika Gupta, who's undergraduate research provided preliminary
426 data used in our experimental design. We also would like to acknowledge Tyler Earp for
427 preparing and analyzing low throughput whole genome bisulfite sequencing data.

428 **Competing Interests**

429 The authors have no competing interests in regards to this work.
430

431 **References**

432 Amukamara A.U., J. T. Washington, Z. Sanchez, E.C. McKinney, A. J. Moore, R. J.
433 Schmitz, P. J. Moore. More than DNA methylation: does pleiotropy drive the complex
434 pattern of evolution of Dnmt1? *Frontiers in Ecology and Evolution* 8, 4 (2020).

435 Bewick, A.J., K. J. Vogel, A. J. Moore, R. J. Schmitz. Evolution of DNA methylation across
436 insects. *Molecular Biology and Evolution* 34, 654-66 (2016).

437 Bewick, A.J., Z. Sanchez, E. C. Mckinney, A. J. Moore, P. J. Moore, R. J. Schmitz. *Dnmt1* is
438 essential for egg production and embryo viability in the large milkweed bug,
439 *Oncopeltus fasciatus*. *Epigenetics & Chromatin* 12, 6 (2019).

440 Chesebro, J., S. Hrycaj, N. Mahfooz, A. Popadić. Diverging functions of Scr between
441 embryonic and post-embryonic development in a hemimetabolous insect, *Oncopeltus*
442 *fasciatus*. *Developmental Biology* 329, 142-151 (2009).

443 Comings, D.E., T. A. Okada. Holocentric chromosomes in *Oncopeltus*: kinetochore plates
444 are present in mitosis but absent in meiosis. *Chromosoma* 37, 177-192 (1972).
445 https://doi.org/10.1007/BF00284937

446 Cunningham, C.B., L. Ji, R. A. W. Wiberg, J. Shelton, E. C. McKinney, D. J. Parker, R. B.
447 Meagher, K. M. Benowitz, E. M. Roy-Zokan, M. G. Ritchie, S. J. Brown, R. J.
448 Schmitz, A. J. Moore. The genome and methylome of a beetle with complex social
449 behavior, *Nicrophorus vespilloides* (Coleoptera: Silphidae). *Genome Biology and*
450 *Evolution* 7, 3383-3396 (2015).

451 Dallai, R. Overview on spermatogenesis and sperm structure of Hexapoda. *Arthropod*
452 *Structure & Development* 43, 257-290 (2014). https://doi.org/10.1093/gbe/evy066

453 Eberhart, C.G., J. Z. Maines, S. A. Wasserman. Meiotic cell cycle requirement for a fly
454 homologue of human Deleted in Azoospermia. *Nature* 381, 783-785 (1996).

455 Economopoulos, A.P. H. T. Gordon. Growth and differentiation of the testes in the large
456 milkweed bug, *Oncopeltus fasciatus* (Dallas). *Journal of Experimental Zoology* 177,
457 391-405 (1971).

458 Ewen-Campen, B., T. E. Jones, C. G. Extavour. Evidence against a germ plasm in the
459 milkweed bug *Oncopeltus fasciatus*, a hemimetabolous insect. *Biology Open* 2, 556-
460 568 (2013).

461 Gegner, J., T.Gegner, H. Vogel, A. Vilcinskas. Silencing of the DNA methyltransferase 1
462 associated protein 1 (DMAP1) gene in the invasive ladybird *Harmonia axyridis* implies
463 a role of the DNA methyltransferase 1-DMAP1 complex in female fecundity. *Insect*
464 *Molecular Biology* 29, 148-159 (2020). https://doi.org/10.1111/imb.12616

465 Glastad, K.M., B. G. Hunt, M. A. Goodisman. Epigenetics in insects: genome regulation and
466 the generation of phenotypic diversity. *Annual Review of Entomology* 64, 185-203
467 (2019). doi.org/10.1146/annurev-ento-011118-111914

468 Hans, F., S. Dimitrov. Histone H3 phosphorylation and cell division. *Oncogene* 20, 3021-
469 3027 (2001).

470 Kay. S., D. Skowronski, B. G. Hunt. Developmental DNA methyltransferase expression in
471 the fire ant Solenopsis invicta. Insect Science 25, 57-65 (2018).

472 Lewis S.H., L. Ross, S. A. Bain, E. Pahita, S. A. Smith, R. Cordaux, et al. Widespread
473 conservation and lineage-specific diversification of genome-wide DNA methylation
474 patterns across arthropods. *PLoS Genetics* 16, e1008864 (2020).
475 https://doi.org/10.1371/journal.pgen.1008864

476 Livak, K.J., T. D. Schmittgen. Analysis of relative gene expression data using real-time
477 quantitative PCR and the 2− ΔΔCT method. *Methods* 25, 402-408 (2001).

478 Lyko, F. The DNA methyltransferase family: a versatile toolkit for epigenetic regulation.
479 *Nature Reviews Genetics* 19, 81-92 (2018).

480 Medrano, J.V., C. Ramathal, H. N. Nguyen, C. Simon, R. A. Reijo Pera. Divergent RNA-
481 binding proteins, DAZL and VASA, induce meiotic progression in human germ cells
482 derived in vitro. *Stem cells* 30, 441-451 (2012).

483 Meinzer, F., S. Dobler, A. Donath, J. N. Lohr. Robust reference gene design and validation
484 for expression studies in the large milkweed bug, *Oncopeltus fasciatus*, upon cardiac
485 glycoside stress. *Gene* 710, 66-75 (2019).

486 Prigent, C. S. Dimitrov. Phosphorylation of serine 10 in histone H3, what for?. *Journal of*
487 *Cell Science* 116, 3677-3685 (2003).

488 Provataris, P., K. Meusemann, O. Niehuis, S. Grath, B. Misof. Signatures of DNA
489 methylation across insects suggest reduced DNA methylation levels in holometabolan.
490 *Genome Biology and Evolution* 10, 1185-1197 (2018).

491 Robinson, K.L., D. Tohidi-Esfahani, F. Ponton, S. J. Simpson, G. A. Sword, N. Lo.
492 Alternative migratory locust phenotypes are associated with differences in the
493 expression of genes encoding the methylation machinery. *Insect Molecular Biology* 25,
494 105-115 (2016).

495 Schmidt, E. D., E. Sehn, A. Dorn. Differentiation and ultrastructure of the spermatogonial
496 cyst cells in the milkweed bug, *Oncopeltus fasciatus*. *Invertebrate Reproduction &*
497 *Development* 42, 163-178 (2002). DOI:10.1080/07924259.2002.9652773

498 Schmitz, R. J., Z. A. Lewis, M. G. Goll. DNA methylation: shared and divergent features
499 across eukaryotes. *Trends in Genetics* 35, 818-827 (2019).
500 doi.org/10.1016/j.tig.2019.07.007

501 Schmitz, R.J., Y. He, O. Valdés-López, S. M. Khan, T. Joshi, M. A. Urich, J. R. Nery, B.
502 Diers, D. Xu, G. Stacey, J. R. Ecker. Epigenome-wide inheritance of cytosine
503 methylation variants in a recombinant inbred population. *Genome Research* 23, 1663-
504 1674 (2013).

505 Schultz, M.D., R. J. Schmitz, J. R. Ecker. 'Leveling' the playing field for analyses of single-
506 base resolution DNA methylomes. *Trends in Genetics* 28, 583-585 (2012).
507 DOI:https://doi.org/10.1016/j.tig.2012.10.012

508 Schulz, N.K., C. I. Wagner, J. Ebeling, G. Raddatz, M. F. Diddens-de Buhr, F. Lyko, J.
509 Kurtz. Dnmt1 has an essential function despite the absence of CpG DNA methylation

510 in the red flour beetle *Tribolium castaneum*. *Scientific Reports* 8, 1-10 (2018).
511 https://doi.org/10.1038/s41598-018-34701-3

512 Shah, C., M. J. VanGompel, V. Naeem, Y. Chen, T. Lee, N. Angeloni, Y. Wang, Y. E. Y.
513 Xu. Widespread presence of human BOULE homologs among animals and
514 conservation of their ancient reproductive function. *PLoS Genetics* 6, e1001022 (2010).
515 doi.org/10.1371/journal.pgen.1001022

516 Tanaka, S.S., Y. Toyooka, R. Akasu, Y. Katoh-Fukui, Y. Nakahara, R. Suzuki, M.
517 Yokoyama, T. Noce. The mouse homolog of Drosophila Vasa is required for the
518 development of male germ cells. *Genes & Development* 14, 841-853 (2000).

519 Ulrich, M. S., J. R. Nery, R. Lister, R. J. Schmitz, J. R. Ecker. MethylC-seq library
520 preparation for base-resolution whole-genome bisulfite sequencing. *Nature Protocols*
521 10, 475–483 (2015). doi: 10.1038/nprot.2014.114

522 Viera, A., J. Page, J. Rufas. Inverted meiosis: the true bugs as a model to study. In:
523 Benavente, R., Volff J.-N. (eds): Meiosis. Genome Dynamics, Basel, Karger, 2009, vol
524 5, pp 137-156 (2009). https://doi.org/10.1159/000166639

525 Yajima, M., G. M. Wessel. The multiple hats of Vasa: its functions in the germline and in
526 cell cycle progression. *Molecular reproduction and development* 78, 861-867 (2011)

527 Zemach, A., I. E. McDaniel, P. Silva, D. Zilberman. Genome-wide evolutionary analysis of
528 eukaryotic DNA methylation. *Science* 328, 916-919 (2010).

529 Zhang, J. Y. Xing, Y. Li, C. Yin, C. Ge, F. Li. DNA methyltransferases have an essential role
530 in female fecundity in brown planthopper, Nilaparvata lugens. Biochemical and
531 Biophysical Research Communications 464, 83-88 (2015).

532 Zwier, M. V., E. C. Verhulst, R. D. Zwahlen, L. W. Beukeboom, L. van de Zande. DNA
533 methylation plays a crucial role during early Nasonia development. *Insect Molecular*
534 *Biology* 21, 129-138 (2012).
535

536 **Figure Legends**

537 **Figure 1.** Progression of spermatogenesis in *O. fasciatus*. In *O. fasciatus* spermatogenesis
538 progresses from the tip of the testis tubule. (A) Dapi-stained testis tubule of stock male. (B)
539 Diagram of the stages of spermatogenesis. At the apical tip (region I) of each of the seven testis
540 tubules there is a "rosette" of niche cells (blue) surrounded by the germline stem cells (B, green;
541 Schmidt et al. 2002). The rosette is not typically visible in confocal images of testis tubules and
542 markers for the rosette have not been identified yet. As spermatogonia (B, light gray) arise from
543 division of the germline stem cells, they are enclosed by cyst cells (B, yellow). In region II,
544 spermatogonia undergo mitotic transit amplification divisions to form spermatocysts containing
545 64 spermatogonia (Economopoulos & Gordon 1971, Ewen-Campen et al. 2013). Spermatocytes
546 (B, dark gray) in region III divide meiotically. *Oncopeltus fasciatus* undergoes inverted meiosis
547 (Viera et al. 2009). Primary spermatocytes undergo the first meiotic division to produce diploid
548 secondary spermatocytes. The meiotic division of the secondary spermatocytes produce the
549 haploid spermatids (B, dark blue) in region IV that then differentiate into spermatozoa in the
550 region V at the terminal end of the testis tubule.

551 **Figure 2**. Expression pattern of *Dnmt1* within the developing testes mirrored that the two
552 gametogenesis genes *Boule* and *Vasa*. *Dnmt1* expression (A) was highest in the larval stages
553 where spermatogenesis is initiated compared to the testes of newly emerged (day 0) and virgin
554 sexually mature (day 7-10) adults. This is similar to the expression patterns of *Boule* (B), in
555 which expression was higher in the 4th and 5th larval stages during which the transition to meiosis
556 occurs compared to newly emerged and virgin sexually mature adults. Expression of *Vasa* (C)
557 demonstrated a similar pattern, with the highest expression in the 4th instar stage and lowest in
558 sexually mature virgin males. Black dots and bars represent mean and SE. Grey dots represent

559 data points for each individual tested. Lower case letters designate significant differences ($p <$
560 0.05) among pairwise comparisons using *post-hoc* Tukey-Kramer HSD test.

561 **Figure 2-figure supplement 1.** Expression of *Dnmt1* is highest in reproductive tissue. As has
562 been seen for females (Amukamara et al. 2020), expression of *Dnmt1* varied across the type of
563 tissue in males.. As in females, expression was lowest in the gut and head compared to the other
564 somatic tissue tested, muscle. Expression is highest in the gonad (testes). Lower case letters
565 designate significant differences ($p < 0.02$) among pairwise comparisons using *post-hoc* Tukey-
566 Kramer HSD test.

567 **Figure 3.** Expression of *Dnmt1* was reduced in the testes of adult males treated with ds-*Dnmt1* at
568 both stages of development. Relative gene expression is standardized to expression levels in
569 control treatments. Black dots and bars represent mean and SE. Grey dots represent data points
570 for each individual tested.

571 **Figure 3-figure supplement 1**. Knockdown of *Dnmt1* (magenta bars), but not *Boule* (blue bars),
572 reduced DNA methylation compared to controls (green bars). Each bar represents a single
573 individual. Across all individuals, the percent methyl CpG is reduced in the DNA isolated from
574 the adult testis of males treated with *ds-Dnmt1*. Earlier injection reduces the percent methylation
575 to a greater extent, consistent with more rounds of cell division within the testes between
576 injection and dissection

577 **Figure 4.** Downregulation of *Dnmt1* during the 3rd instar stage of development significantly
578 reduced the size of the testis in sexually mature males. There was no effect of downregulation of
579 *Dnmt1* on testis size when treatment occurred during the 5th instar stage of development after
580 meiosis has been initiated. Black dots and bars represent mean and SE. Grey dots represent data
581 points for each individual tested.

582 **Figure 5**.

583 Timing of treatment during development determined the effect on testis structure of adults that
584 develop from *Dnmt1* (Panels B and D) knockdown males. In control testis tubules from males
585 injected with ds-RED (A and C), spermatogonia divided mitotically in region II to form
586 spermatocysts as is observed in untreated males. Mitotic spermatogonia are labeled with anti-
587 phosophohistone 3 antibodies in region II of the testis tubule (C, arrowhead). Meiotic divisions
588 also occured as in untreated males in ds-RED injected males. In our ds-RED control samples, a
589 band of synchronously dividing spermatocysts, identified by positive anti-phosphohistone H3
590 antibody staining, was present at the interface between primary and secondary spermatocytes (A,
591 C). In testes from males with *Dnmt1* knockdown in the 3rd instar (B), the anterior tip of the testis
592 tubule showed evidence of mitotic activity (arrowhead). However, there were fewer
593 spermatocytes present and the spermatocysts in this region were disorganized and there was little
594 evidence of the band of positive anti-phosphohistone H3 stained meiotic spermatocytes. The
595 testis tubule structure from males treated with ds-*Dnmt1* following meiosis at the 5th instar stage
596 of development (D) was more similar to the controls than those treated at the 3rd instar stage of
597 development. In ds-*Dnmt1* males treated at the 5th instar stage, there were positive anti-
598 phosphohistone H3 stained spermatogonia (arrowhead) and spermatocytes (arrow). There were
599 differences between males treated as 5th instars with ds-RED males and ds-*Dnmt1*, however,
600 including spermatocysts containing cells with highly condensed nuclei that were not present in
601 the controls and fewer spermatocysts containing spermatids or spermatozoa. All images taken at
602 10X magnification.

603 **Figure 5-figure supplement 1**. *Boule* knockdown with RNAi showed the expected phenotype in
604 males. (A) ds-*Boule* RNA treatment reduced *Boule* expression compared to ds-RED injected

605 males. Black dots and bars represent mean and SE. Grey dots represent data points for each
606 individual tested. (B) While the anterior end of the testis tubule in *Boule* knockdown males
607 treated at the 3rd instar stage of development look relatively normal, with spermatogonia dividing
608 normally (B, arrowhead), RNAi resulted in a failure to produce spermatozoa and an abnormal
609 phenotype in region IV. While there was some evidence of anti-phosophohistone 3 staining in
610 spermatocytes (B, arrow), it was reduced and did not mark a transition between spermatocytes
611 and spermatids as is seen in control males. (C) A similar phenotype is seen in males treated with
612 ds-*Boule* RNA at the 5th instar stage of development. 10X magnification.
613 **Figure 6**. Females mated to control males lay fertilized eggs longer than females mated to
614 *Dnmt1* knockdown males. Eggs were collected twice per week and eggs allowed to develop to
615 hatching. Eggs that did not hatch showed no sign of development, indicating that they had not
616 been fertilized. Both treatments demonstrate a decrease in proportion of eggs that hatch over
617 time, but the ds-*Dnmt1* treatment group shows a faster decrease.
618 **Figure 6-figure supplement 1:** Downregulation of *Dnmt1* in sexually mature males resulted in a
619 loss of testis area following multiple matings. Control males allowed to mate with multiple
620 females across three weeks had larger testes than males treated with ds-*Dnmt1* at sexual
621 maturity. Black dots and bars represent mean and SE. Grey dots represent data points for each
622 individual tested.
623 **Figure 7**. Testis structure breaks down in *Dnmt1* knockdown males treated as adults after having
624 sperm replenishment induced by mating activity. The regions of spermatogenesis were apparent
625 in mated males following 3 weeks of mating activity in control testis tubules (A and B) and the
626 evidence of both mitotic division in spermatogonia (B, arrowhead) and the band of meiotic
627 divisions was clear from anti-phosphohistone H3 staining. In *Dnmt1* knockdown males at low

628 magnification (C), the anterior tip of the testis tubule looked relatively normal. However, the
629 region containing both the primary and secondary spermatocytes was disorganized.
630 Spermatocyst structure was broken down, and the nuclei of the primary and secondary
631 spermatocytes had lost their characteristic structure (Ewen-Campen et al. 2013). Finally, there
632 were fewer mature spermatids in the posterior end of the testis tubule. At higher magnification
633 (D), it was apparent that nuclear structure in the anterior tip was also affected by the knockdown,
634 both in the spermatogonia and spermatocytes. Spermatogonia nuclei in the *Dnmt1* knockdown
635 testis tubules (D) were more condensed than in the control testis tubules (B), although they still
636 seemed to be organized into spermatocysts. Spermatocyte nuclei, however, were fewer in
637 number than in controls, did not have their characteristic shape (Ewen-Campen et al. 2013,
638 Economopoulos & Gordon 1971), and were not organized in spermatocytes. A and C:10X
639 magnification, B and D: 20X magnification.
640

641 Figure 1

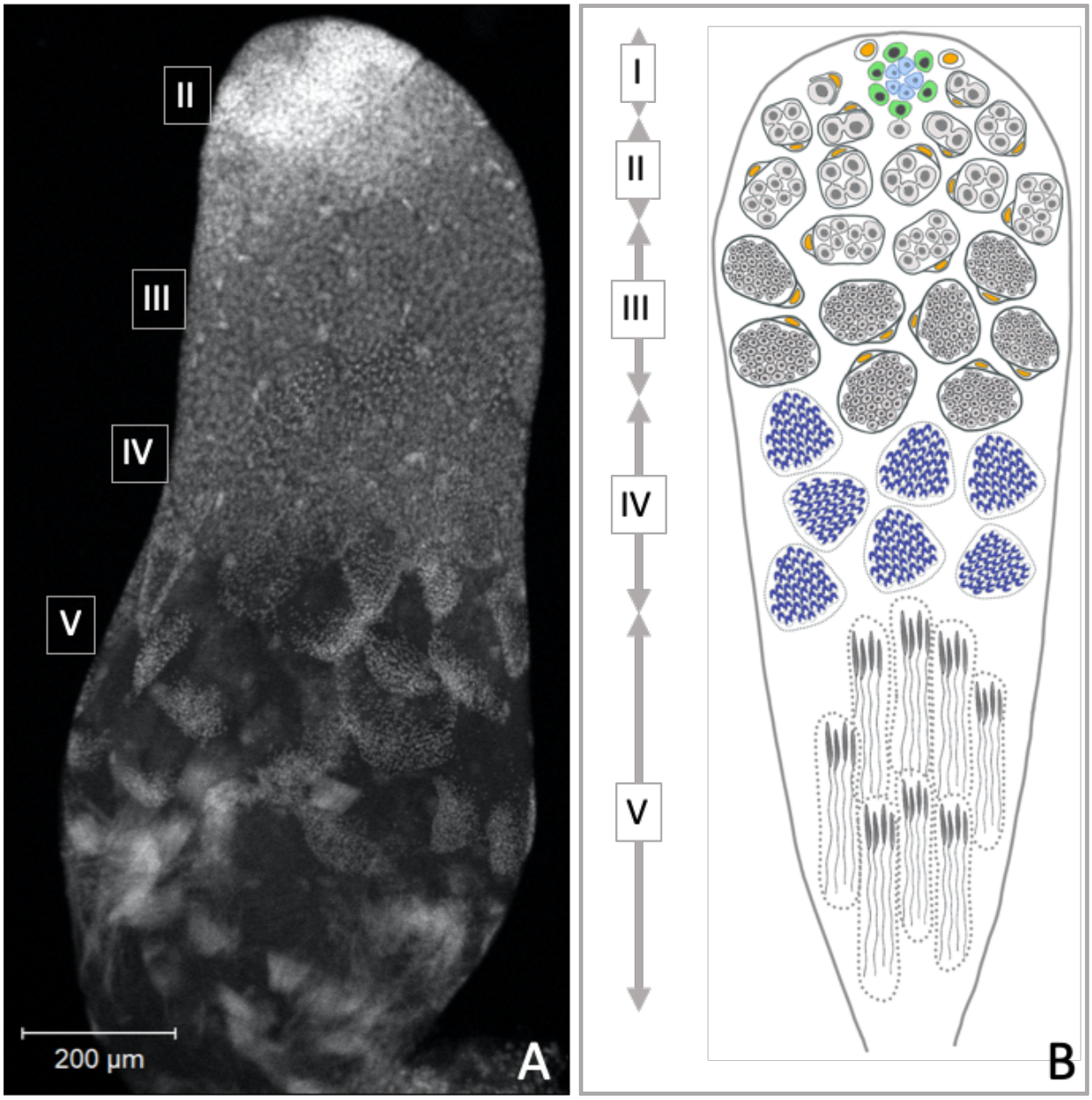

642

643

644 Figure 2.

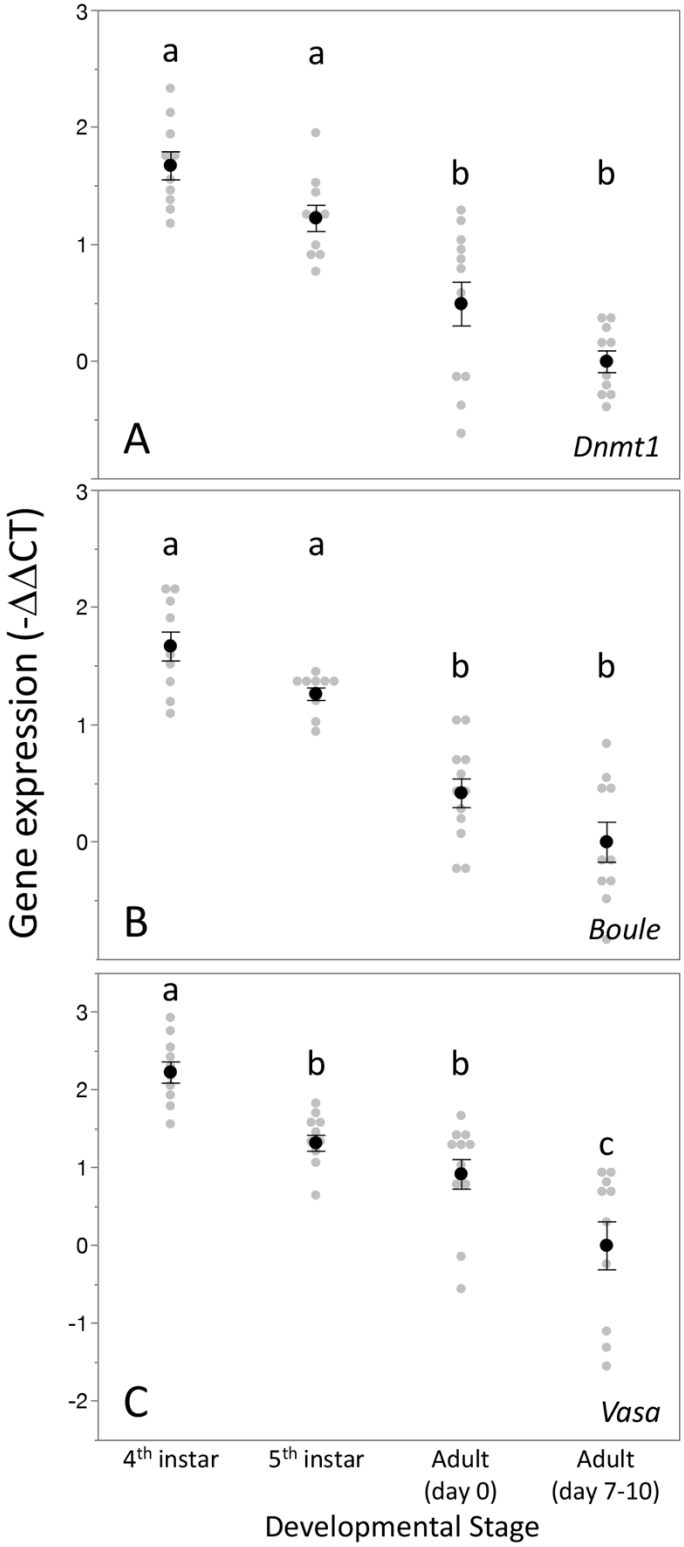

645

646 Figure 2-figure supplement 1.

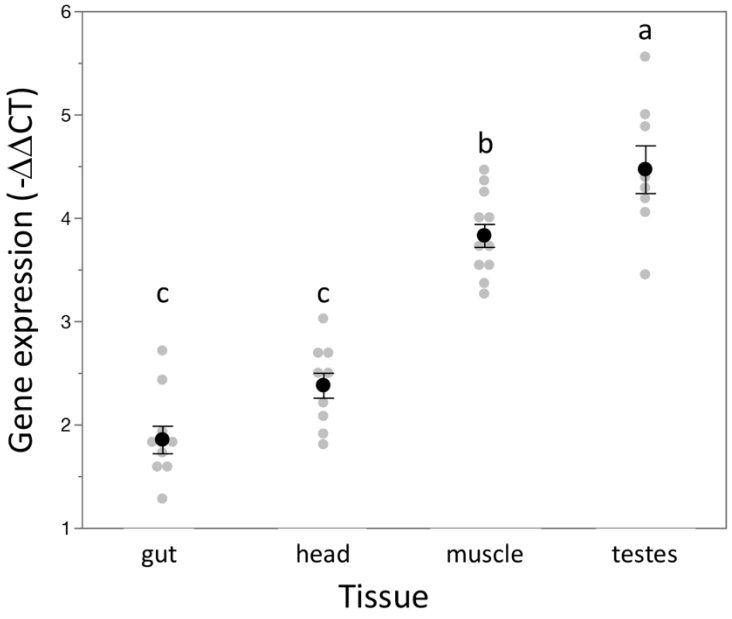

647

648 Figure 3.

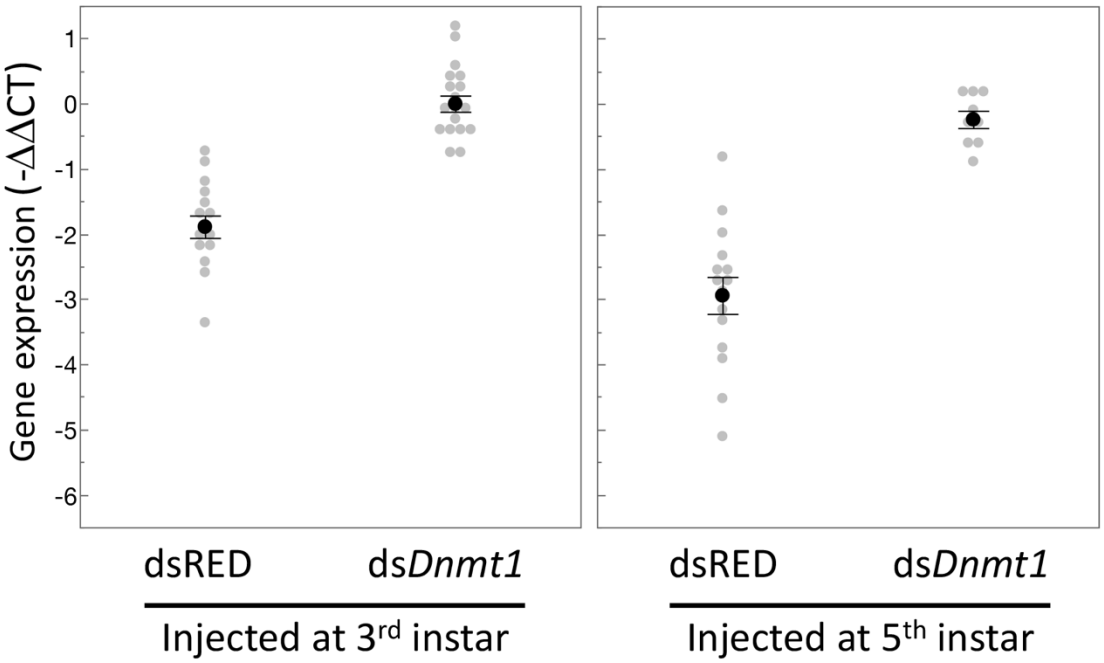

649

650

651

652 Figure 3-figure supplement 1.

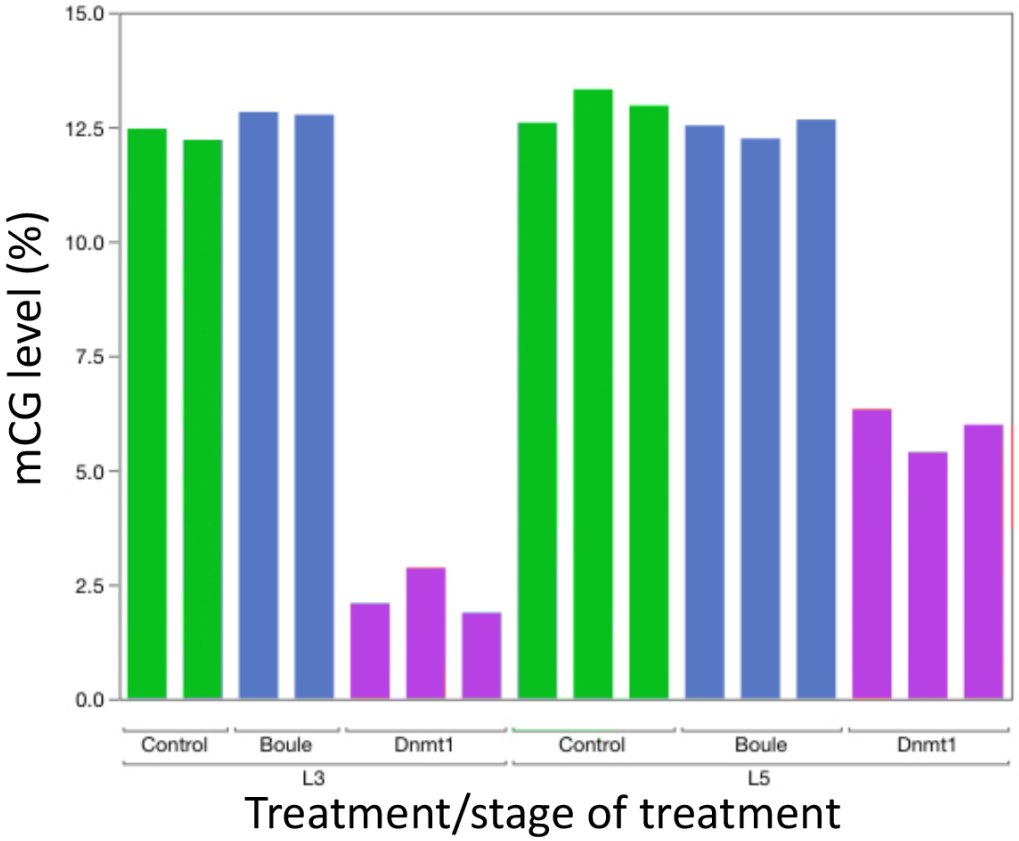

653

654

655 Figure 4.

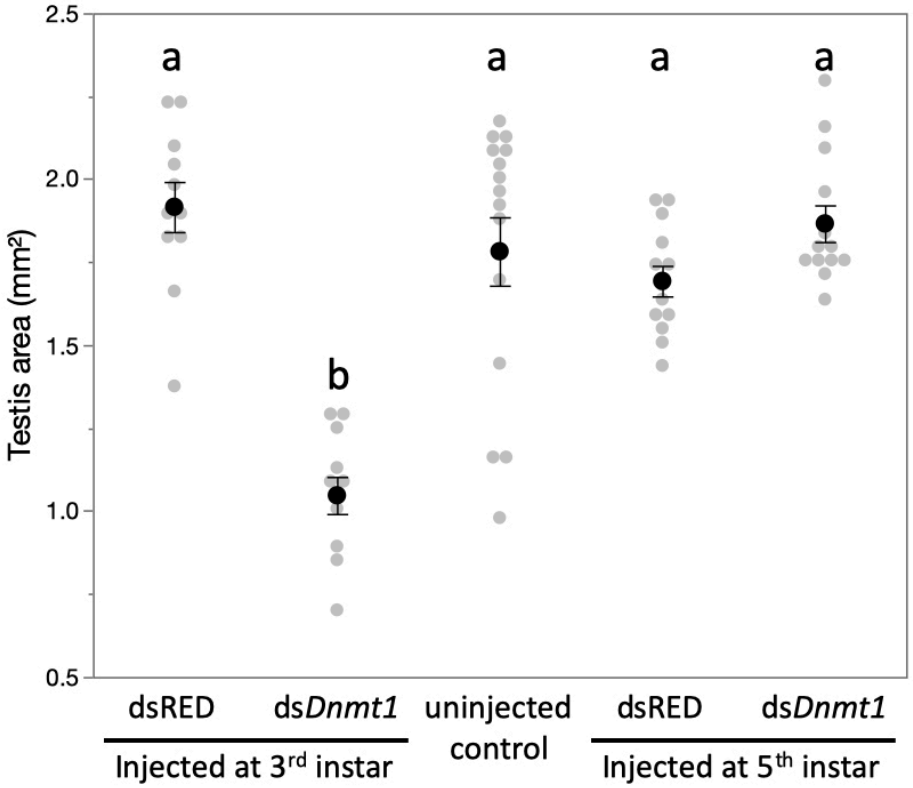

656

657

658 Figure 5.

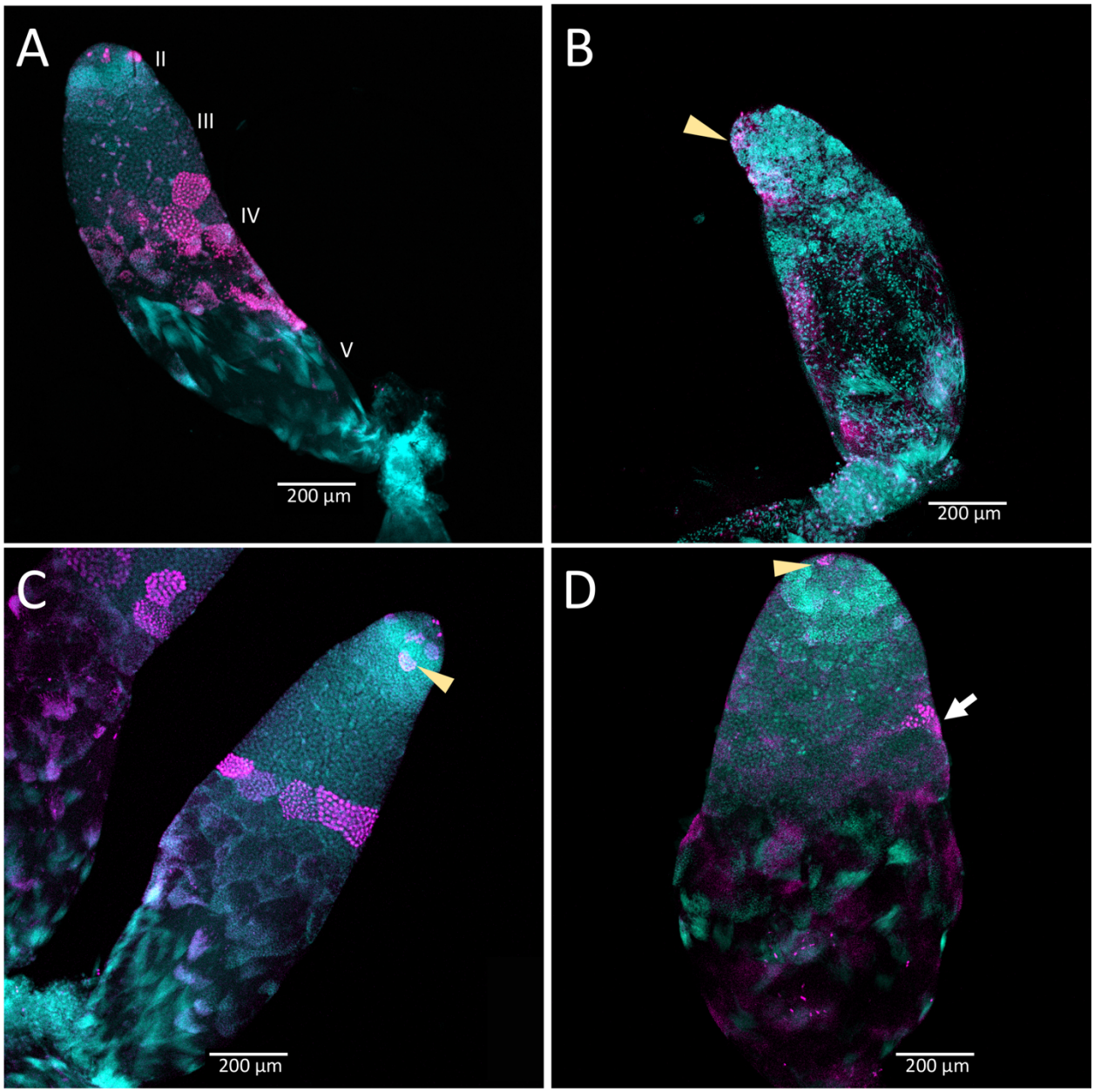

659

660

661 Figure 5-figure supplement 1.

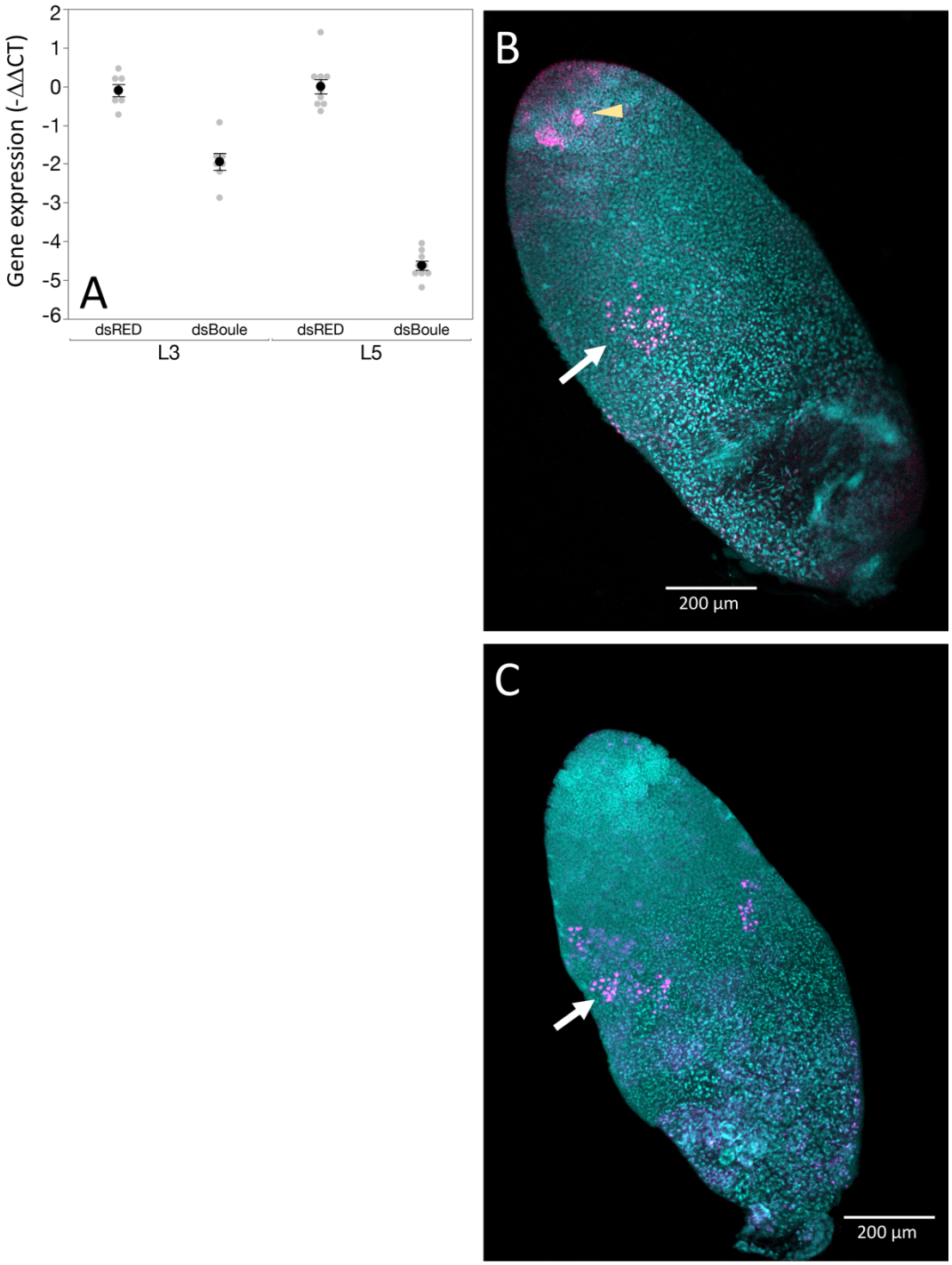

662

663

664

665 Figure 6.

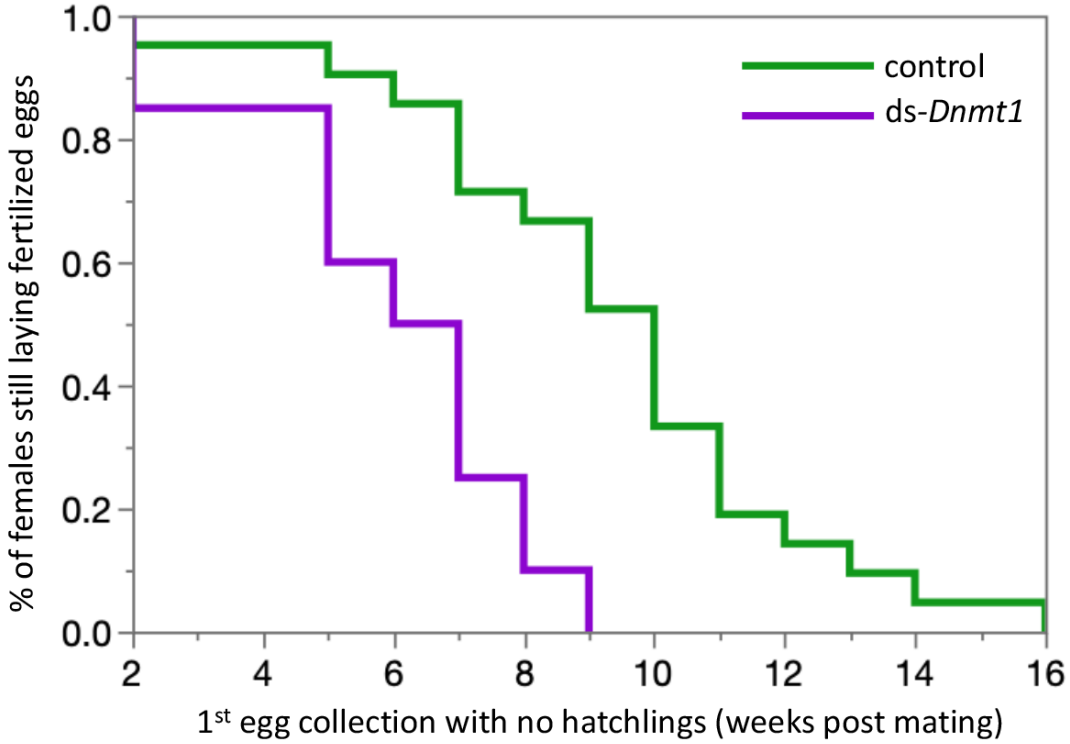

666

667

668 Figure 6-figure supplement 1.

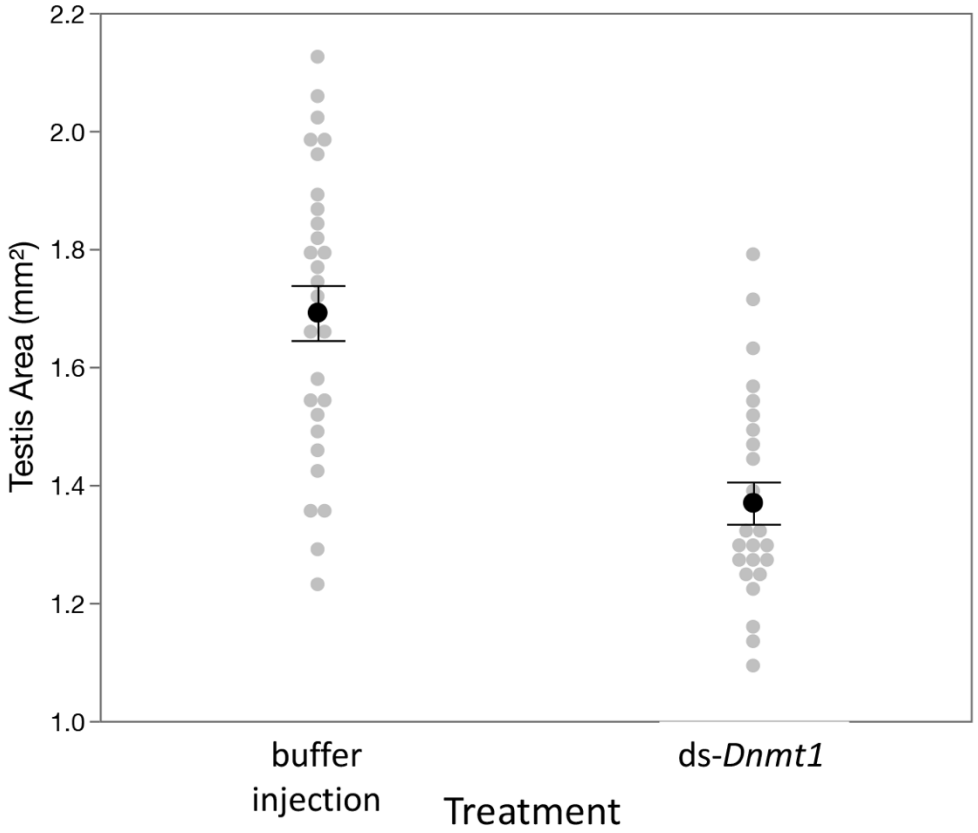

669

670

671 Figure 7.

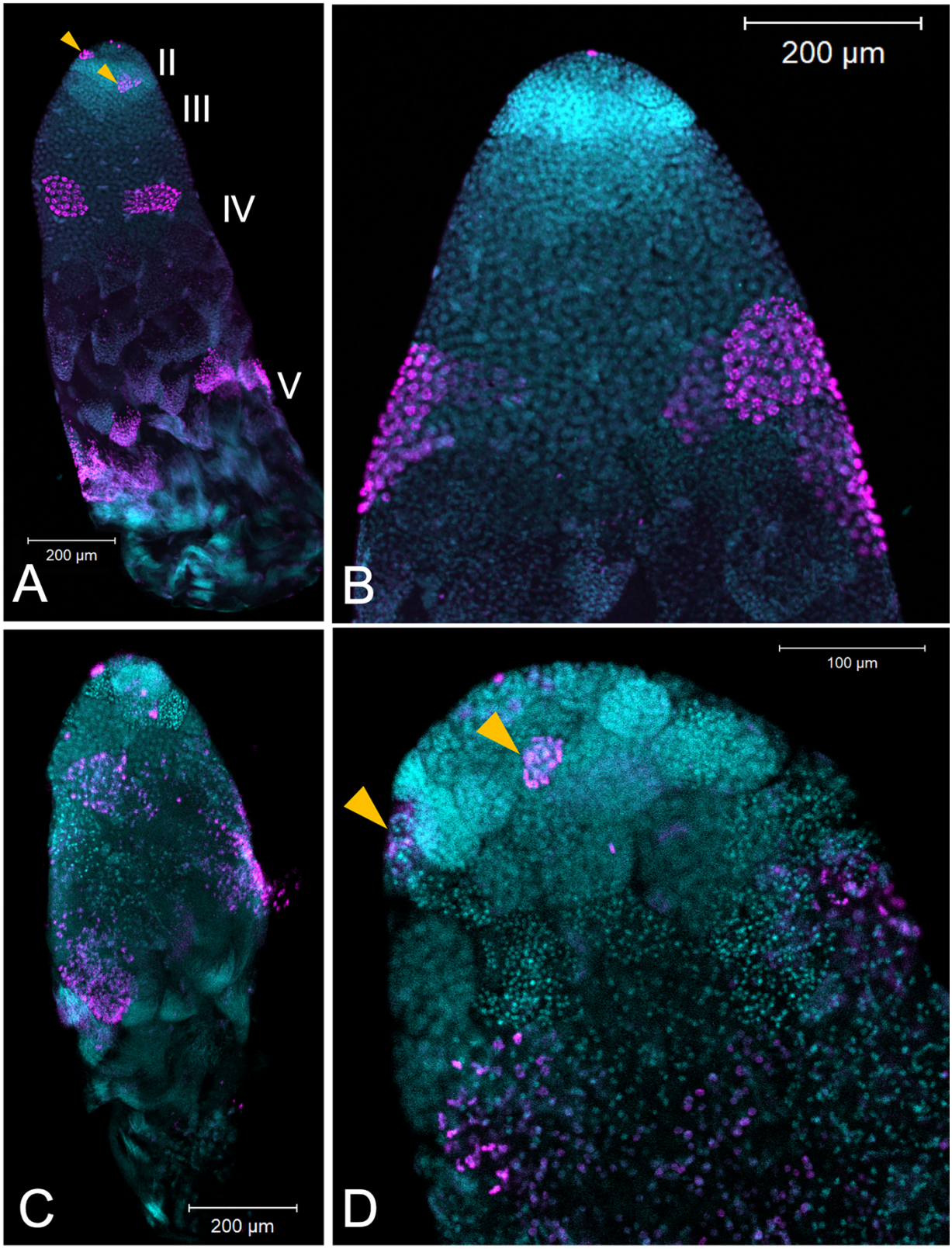

672